Jestr

Journal of Engineering Science and Technology Review 14 (6) (2021) 211 - 219

JOURNAL OF
Engineering Science and Technology Review

Research Article

www.jestr.org

Mapping of Dry Marginal Agricultural Land Occupation and Change Using Landsat-8 and Sentinel-2

Marga Mandala, Indarto Indarto*, Entin Hidayah and Farid Lukman Hakim

Keris P-LSO, LP2M, Universitas Jember, Jl. Kalimantan no. 37 Kampus Tegalboto Jember 68121, Jawa Timur, Indonesia

Received 29 July 2020; Accepted 21 October 2021

Abstract

The abundance of dry marginal agricultural land in Indonesia provides an alternative land resource for crop production. This study uses Landsat 8 and Sentinel-2A satellite imagery to map the spatial extent of such land and to interpret the results obtained to track changes in its use. Supervised classification is used for image processing and the production of land-cover maps. The classified maps produc§ed and the spatial extent of each class are compared to existing maps and statistical data. Regional development by local governments has led to the occupation of a greater area of dry marginal agricultural land, and from 2000 to 2019 about 49% of such land has been occupied and converted to productive land use. This change can be identified as an increase in plantation area and the conversion of non-irrigated or irrigated areas to pavement area. Both Landsat 8 and Sentinel-2A imagery can potentially be used to map the spatial extent of dry marginal agricultural land and the maps produced can be useful for updating incomplete statistical records.

Keywords: mapping, dry-marginal, agricultural-land, Sentinel-2A, Landsat 8.

1. Introduction

Marginal agricultural land (MAL) is defined as land in which conditions are too severe for sustained application and which is sensitive to land degradation. Inappropriate human intervention and contaminated and potentially contaminated sites can cause land degradation [1], [2] and such land is then abandoned and rarely used. However, this land type can be considered as an alternative resource for crops for both food and energy production. Use of MAL for the production of industrial crops to serve biomass and energy demands has been discussed in recent studies [3, 4].

The MAL found in many locations of the Indonesian archipelago. It comprises about 157.2 million ha or 83.13% of the total area of land [5]. According to the Indonesian land resources database, MAL in Indonesia is divided into six categories: (1) acid upland, (2) semiarid upland, (3) tidal swampland, (4) inland swamp, and (5) peatland [6]. Mulyani and Sarwani [5] state that 108.8 million ha of land is classified as acid upland, distributed mainly in Sumatra, Kalimantan and Papua. In contrast, semiarid uplands cover an area of 13.3 million ha distributed across East Kalimantan, East Java, Bali, West Nusa Tenggara and East Nusa Tenggara.

Semiarid soil [7] and semiarid uplands [5] are defined as soil/land having specific regimes of soil moisture in specific dry-climate conditions. Rainfall in semiarid areas is usually no more than 2000 mm per year, and the dry-month period (defined as months receiving rainfall of less than < 100 mm [5]) can exceed seven months [6]. In this study, we use the term 'DryMAL' (dry marginal agricultural land) to represent semiarid uplands [5] and semiarid soils [7]. These three terminologies are largely similar in that they describe MAL that is relatively dry because of intrinsic or external factors.

EUROSTAT [8] defines land cover (LC) as 'corresponding to a physical description of space' that 'enables various biophysical categories to be distinguished', observations of which can come from sources such as 'the human eye, aerial photographs, [and] satellite sensors'. Meanwhile, the term 'land use' (LU) refers to 'areas in terms of their socio-economic purpose: areas used for residential, industrial or commercial purposes, for farming or forestry, for recreational or conservation purposes'. Similar definitions are proposed by Parece [9], and so in this paper, we use the definitions and abbreviations above to describe land cover and land use (LCLU).

Many efforts have been initiated to increase productivity and to reduce the obstacles to DryMAL use and, to this end, mapping to calculate the spatial extent of this land resource is urgently required. This study aims to evaluate the application of Sentinel-2A and Landsat 8 imagery for mapping the spatial extent of DryMAL and other land occupations, both to compare the classification results with existing maps and statistical data and to detect the change in DryMAL occupation between 2000 and 2019.

2. State of the Art

Satellite imagery promises solutions for many problems in the field of agriculture. Sentinel-2A and Landsat 8 imageries are available for free download, and these two global-coverage remote-sensing systems provide rapid, low-cost, easy-to-apply imagery for the end-user. Both Sentinel-2A and Landsat 8 are capable of mapping LCLU at specific times and locations, and thematic mapping obtained from the data provided by these satellites may offer up-to-date LCLU maps for further applications. LCLU maps interpreted from conventional maps or derived from satellite imageries have been applied to the study of LCLU changes [10], [11].

*E-mail address: indarto.ftp@unej.ac.id
ISSN: 1791-2377
doi:10.25103/jestr.146.24

Furthermore, Fonji and Taff [12] have combined current data (census and statistics) with satellite imagery (Landsat Thematic Mapper) to calculate LCLU change in north-eastern Latvia. Other researchers seek to explore the causal effects of LCLU and their implications for society and the environment [13], [14]. Further studies have attempted to integrate data using fusion techniques or to combine data with a more comprehensive study of LCLU phenomena [15], [16]. Furthermore, the use of Landsat imagery as a method for studying LCLU change across the globe is both widely known and widely published [17], [18], [19]. In parallel, the application of Sentinel-2A imagery for the interpretation of LCLU has also becoming popular in research over the last five years. Some examples of the use of Sentinel-2A imagery for identification and mapping in agricultural-related issues can be found in studies conducted by Bassa et al. [20], Rujoiu-Mare et al. [21], Forkuor et al. [22], Abdi [23] and Goga et al. [24]. These studies show the potential applicability of Sentinel-2A for mapping LCLU and phenomena related to agriculture.

Both Landsat 8 and Sentinel-2A provide high-spectral-resolution and medium-spatial-resolution imagery potentially applicable to LCLU mapping. The relatively similar properties of these two imageries are useful for researchers wanting to compare or combine satellite data to obtain more comprehensive interpretations. For example, Sertel and Musaoğlu [25] compare the classification accuracy of LC and LU maps created from Sentinel-2 and Landsat 8 imagery, and Degife, Zabel and Mauser [25] examine the rate, extent and distribution of various LU and LC changes in Gambella Regional State, Ethiopia. Furthermore, Mishra and Rai [26] use Landsat 5 TM (Thematic Mapper) and Sentinel-2A MSI (Multispectral Instrument) imagery to extract land-cover maps. The dense time series of Landsat 8 OLI (Operational Land Imager) and Sentinel-2A (or 2B) MSI imagery are creating new opportunities to map and to characterise temporal dynamics in land-surface properties by combining the two imageries [27].

Image classification is defined as the categorising of digital-image pixels into particular land-cover classes or themes. Most image-processing techniques are based on hard logic, utilising both spectral and temporal-spatial patterns. The supervised and unsupervised classification are based on the hard logic technique [28], [29], [30]. Supervised classification can be explored using many algorithms; however, consideration of type, the number of training areas and the selected band combination are critical [31]. Khorram et al. [28] state that the maximum likelihood classification algorithm is the most commonly used method. Finally, many methods of accuracy assessment have been discussed in the remote-sensing literature [32], [33], [34]. The most commonly used method for evaluating the accuracy of image classification uses the confusion matrix with the level of acceptance in a range from 75% to 90%. Finally, Foody [34] recommends the use of a minimum of 89% ± 5% interval of confidence of accuracy assessment for image classification results.

3. Methodology

3.1 Study site

Situbondo regency (Fig.1) is located in the eastern part of East Java and has a total area of 1651.30 km^2. The regency has a total population of 691,622 and a population density of 422 per km^2. Annual population growth rate calculated for 2018–2019 is 0.46% [35].

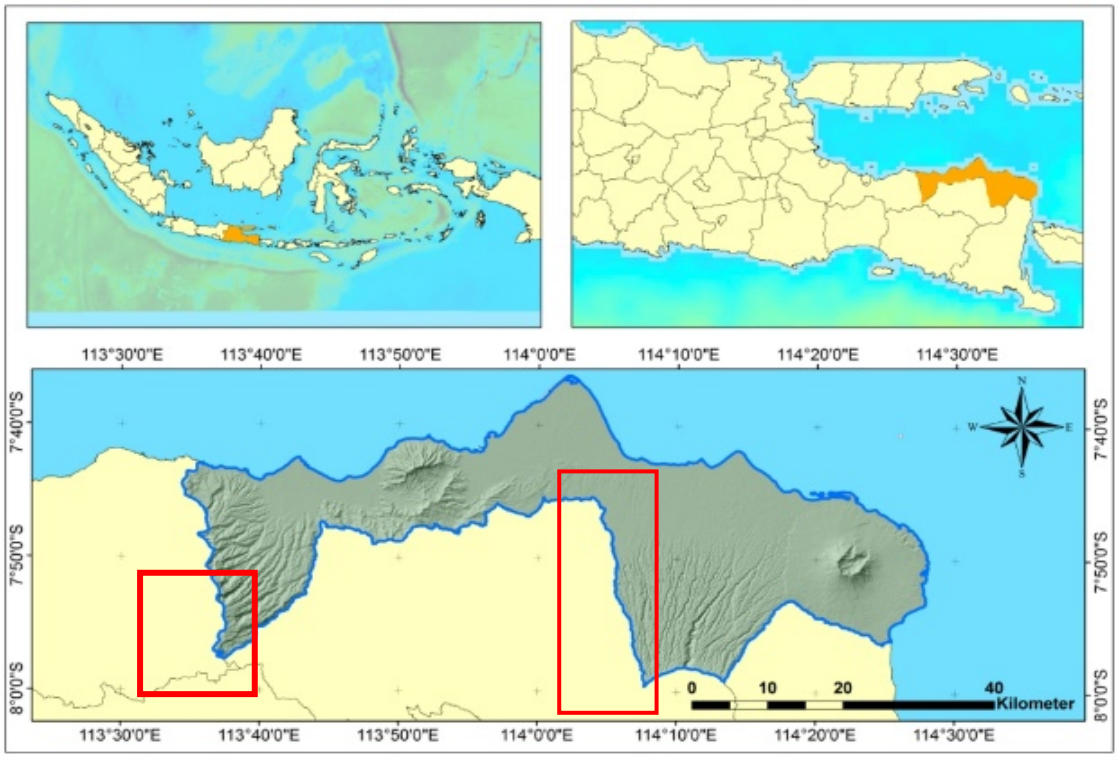

Fig. 1. Study site – Situbondo regency

Situbondo regency is relatively drier than other locations in East Java, with annual rainfall ranging from 500 to 1500 mm; this is less than average annual rainfall in other East Java regions of from 1500 to 3500 mm. The dry season in this region ranges from seven to nine months a year and runs from April/May to November/December. The rainfall received per month is very limited, with more than 100 mm occurring only in the four months from January to April. Thin

layers characterise the soil in this region, with shallow soil and relatively low levels of organic matter.

In many places, gravel mixed with upper soil layers, and this stony soil layer is usually found in higher areas, and those are having slight to moderate slopes. Moreover, macrospores present in the soil layer accelerate runoff infiltrating and percolating more rapidly to the soil layer. As a result, some intermittent rivers flow in this region. The combination of shallow soil layers in stepped terrain drainage, the presence of macrospores and intermittent rivers continuously recharge groundwater resources. The groundwater is, therefore, the primary source of water in this region. Fig. 2 (a, b, c) shows examples of DryMAL photographs obtained from the region and discussed further in this study.

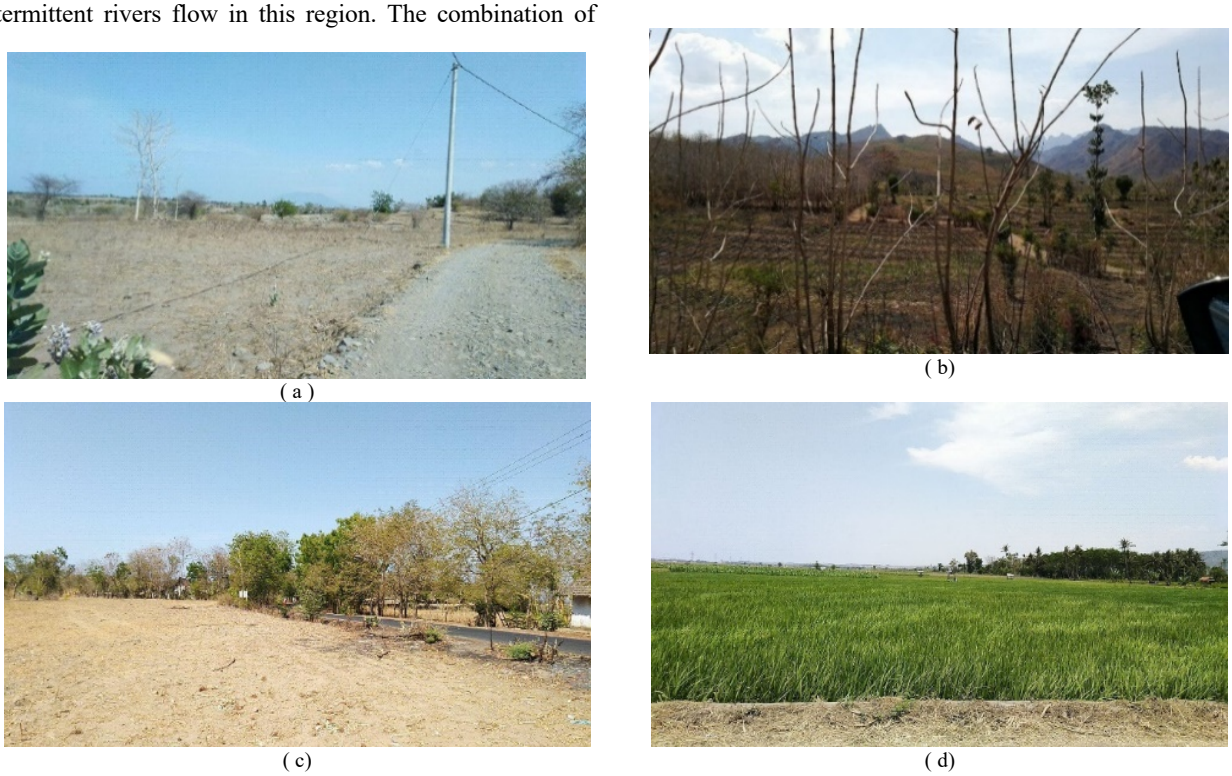

(a) (b) (c) (d)

Fig. 2. Examples of DryMAL (a, b and c) and irrigated paddy field (non-dry land) (d). Photographs were taken in the same week in October 2019.

DryMAL usually has low productivity that is constrained by internal factors, such as parent material of soil, physical and biological properties, and external factors such as rainfall and temperature [5]. Furthermore, because the weathering and destruction of parent material are not as intensive as in wet climates, the formation of soil in DryMAL is relatively reduced. The soil solum is relatively shallow and forms relatively rocky soil with many rock disclosures. The primary materials found in DryMAL are limestone, karst limestone, and sedimentary and volcanic materials. The soil pH is either neutral or tends to be alkaline. DryMAL generally has better fertility than acid upland areas, and common soils types in DryMAL are Alfisols, Mollisols, Entisols and Vertisols [5].

3.2 Input data

Primary input data for this study is Sentinel-2A and Landsat 8 imagery of the location of interest downloaded from the USGS website [36]. The images used are selected based on the minimum cloud cover present (**Fig.3**). Therefore, for Landsat 8, two images for different dates are selected. Table 1 visualises the raw image metadata related to the raw images.

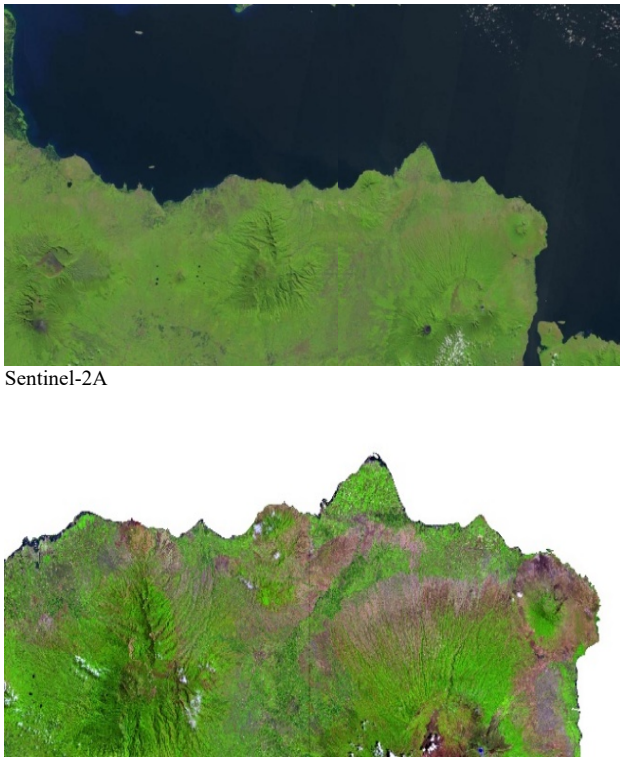

Sentinel-2A

(b) Landsat 8

Fig. 3. Raw image input data

Table 1. Raw image metadata – Sentinel-2A and Landsat 8

Satellite	Date acquired (dd/mm/year)	Cloud cover (%)	Data type/ collection category	Orbit
Sentinel-2A	25/06/2019	0.0179	S2A_MSIL1C	Descending
	25/06/2019	0.1016	S2A_MSIL1C	Descending
Landsat 8	06/11/2016	5.72	L1TP/T1	Ascending
	01/10/2019	9.24	L1TP/T1	Ascending

This study is constrained by the availability of images clear of cloud cover. In tropical regions such as this, it is a challenge to obtain imagery from optical sensors with minimum cloud coverage, and typically the imagery captured in dry seasons is better than in wet seasons. Although imageries downloaded for this study represent the dry season, Sentinel images were captured at the beginning of the season while Landsat images were captured later on in the season. Visually (as shown in Fig. 3) the Sentinel-2A images show more greenness than the Landsat images because of the presence of vegetation remaining from the end of the wet season, and this will probably influence the classification process. Thematic maps known as RBI (Rupa Bumi Indonesia) maps were downloaded from the Indonesian Geospatial Agency (Badan Informasi Geospatial) and used to interpret the classification results [37].

3.3 Tools used

In this study, a MultiSpec© package [38], [39] was used as the tool for image processing, and QGIS [40] was applied for atmospheric correction, pan-sharpening (re-classifier image) and visualisation. Global Positioning System (GPS) was utilised to collect ground control points (GCPs).

3.4 Procedure

The image treatment process **(Fig. 4)** consists of three paths. The left path is applied to produce LCLU maps from Landsat 8 and Sentinel-2A images. Starting with raw Landsat 8 and Sentinel-2A images downloaded from the website [41] the following steps are carried out: atmospheric correction, creation of image composites, field surveys for collecting training areas or GCPs, supervised classification, accuracy assessment using confusion matrix, post-processing, clipping of the maps with regency/district boundaries, and image interpretation.

A dark object subtraction algorithm is exploited to prepare atmospheric correction via the Semi-Automatic Classification Plugin (SCP) [41] provided on the QGIS platform, and the pan-sharpening method is applied in parallel with the atmospheric correction in the SCP. In this study, the pan-sharpening method used is based on that described by Johnson et al. [42].

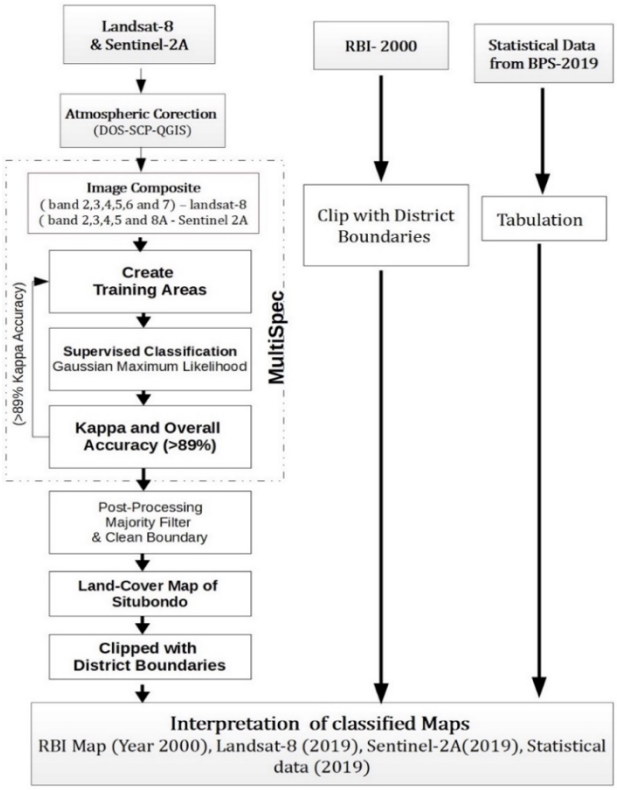

Fig. 4. Procedure

We use five composites bands of Sentinel-2A imagery (bands 2, 3, 4, 5 and 8). The spatial resolution of pixels is 10m, meaning that one pixel on the image represents 10m x 10m on the ground. Then, the Composite bands of Landsat 8 imagery are created by a combination of six bands (Bands 2, 3, 4, 5, 6 and 7). The individual pixels in the Landsat provide spatial resolution at the ground level of 30m. However, in this study, the pan-sharpening method adapted from Johnson et al. [42] can provide Landsat images with 15m pixel size.

Moreover, several field surveys were conducted between May to November 2019 to establish GCPs to determine the real conditions in the field and to take photographs from the region of interest. About 771 GCPs were collected and used as training areas. Table 2 summarises the statistics for the GCPs used for each LCLU class.

Table 2. Collected training areas (GCPs)

Class	Number TA	Area (ha)	Min	Max	Median
Waterbody	40	553.94	1.23	54.30	20.1
Forest/plantation	184	12,366.5	1.78	209.0	77.1
DryMAL	165	4280.21	1.21	93.5	26.6
Non-irrigated land	92	2169.50	1.40	46.8	23.8
Built-up area	140	3425.64	2.38	56.7	21.9
Irrigated paddy fields	150	3222.64	1.14	56.8	23.5
Total	771	26,018.35			

In this study, a Gaussian maximum likelihood algorithm is utilised to perform supervised classification. Khorram et al. [43] state that maximum likelihood classification is commonly exploited for image classification processes. The classification explores the five composites bands of Sentinel-2A imagery, the six bands of Landsat 8 imagery and the 771

GCPs used as training areas. The classification procedure follows existing protocols as detailed by Biehl [39] and Landgrebe [44]. A general confusion matrix is used to assess the accuracy of classification processes using overall and kappa indices [34]. The level of accuracy targeted is 89%, following Foody's recommendation [34].

Furthermore, post-processing treatment is applied to the two maps using the majority filter and clear-boundary tools. The image then clips with a polygon of Situbondo regency, and the two maps are applied for the interpretation. Two different district areas apply for the comparison. In the final step, the two maps (from Sentinel-2A and Landsat 8), the RBI maps and the statistical data are compared and interpreted. In the second path shown in Fig. 4, the clipped map from RBI is applied to visualise LCLU in the year 2000.

The second thematic map, processed from Sentinel-2A, and the third map, classified from Landsat-8, were then used to visualised LCLU in 2019. Finally, in the third path, the statistical data obtained from BPS Situbondo [35] is presented as additional information about LCLU in the region.

4. Results and Discussion

4.1 General results

Tables 3 and 4 present the accuracy per class obtained from Sentinel-2A and Landsat 8 imagery. The reference and reliability accuracy shows the accuracy of classification processes for each class [39].

Table 3. Accuracy of Sentinel-2A images

Class	Reference accuracy (%)	Pavement areas	Irrigated paddy	Non-irrigated land	DryMAL	Water-body	Forest-plantation	Total
Pavement areas	91.04	27587	432	201	2073	1	8	30302
Irrigated paddy	97.85	175	21941	0	234	0	74	22424
Non-irrigated land	91.56	20	763	8843	32	0	0	9658
DryMAL	97.80	2187	234	763	141510	0	0	144694
Waterbody	99.76	10	1	0	0	4621	0	4632
Forest-plantation	99.82	103	110	0	0	0	116328	116541
Total		30082	23481	9807	143849	4622	116410	328251
Reliability accuracy (%)		91.71	93.44	90.17	98.37	99.98	99.93	

Table 4. Accuracy of Landsat 8 images

Class	Reference accuracy (%)	Pavement areas	Irrigated paddy	DryMAL	Waterbody	Forest-plantation	Total
Pavement areas	94.75	43508	0	2409	0	0	45917
Irrigated paddy	98.86	730	82271	0	0	219	83220
DryMAL	96.22	2628	0	66941	0	0	69569
Waterbody	99.08	3	146	100	26937	0	27186
Forest/plant-ation	97.99	73	2847	0	0	142350	145270
Total		46942	85264	69450	26937	142569	371162
Reliability accuracy (%)		92.68	96.49	96.39	100	99.85	

The two tables show that individual accuracy for each class is greater than the 89% threshold [34]. In general, we can, therefore, state that individual accuracy for each class, overall and kappa accuracy meet the standard classification processes. Sentinel-2A imagery can separate the features into six significant classes. In comparison, Landsat classified features only into five classes, the difference being in the class of 'non-irrigated land'. In this region of interest, both non-irrigated land and DryMAL refer to the same features, that is Land not reached by irrigation infrastructure and relatively dry due to intrinsic or external factors [5], [7]. The term 'non-irrigated land' refers more to land-use, while the term 'DryMAL' refers to land-cover.

Classification Sentinel-2A image produces an overall and kappa accuracy of **97.74%** and **96.61%.** In Landsat 8, the classification produces overall and kappa accuracy of **97.53%** and **96.68%,** respectively. According to Foody [34], the classified maps above is satisfier. The two tables also indicate that both Sentinel-2A and Landsat 8 perform best for the classification of five classes (pavement area, irrigated-paddy, DryMAL, waterbody and forest/plantation), meaning that both imageries can identify and distinguish these features.

Fig. 5 shows the results of classification, and Table 5 presents the comparison of area extent in km^2 and the percentage of the total area for each type of LCLU.

However, misinterpretation still exists between pavement areas and DryMAL, meaning that in some places both Landsat 8 and Sentinel-2A have difficulties in distinguishing between these types of LCLU. This is probably due to the relatively similar spectral properties of house roofs and DryMAL; the majority of house roofs are produced from pre-casts of specifics soil type, and therefore appear in the imageries as spectrally similar to DryMAL. Otherwise, this misinterpretation may be caused by confusion between pixel size and ground-feature size. The spatial resolution of Landsat 8 pixels is 15m x 15m and for Sentinel-2A is 10m x 10m. In the field, the majority of individual building sizes, both in rural and urban areas, range between 5 and 30 metres. As result, an area composed of a mix of DryMAL and pavement, pixels will be classified as DryMAL or pavement depending on which is the majority cover.

The three maps can potentially be used to describe LCLU change from 2000 to 2019, with change being observed using three classes, i.e. DryMAL, forest-plantation, and non-

irrigated areas. The original land resources from which these three classes are formed are similar, i.e. DryMAL. The area occupied by these three classes in the RBI map (Table 5) is 80.6% of the total area (52% + 22% + 6.6%, respectively). In the Landsat 8 map, the areas for the same classes is 70.9% (32.2% + 38.7% + 0%, respectively), while in the Sentinel-2A map, the area occupied by DryMAL, forest/plantation and non-irrigated land is 76.9% (26.3% + 49.5% + 1.1%, respectively). These percentages indicate the original extent in the area of DryMAL resources in the region.

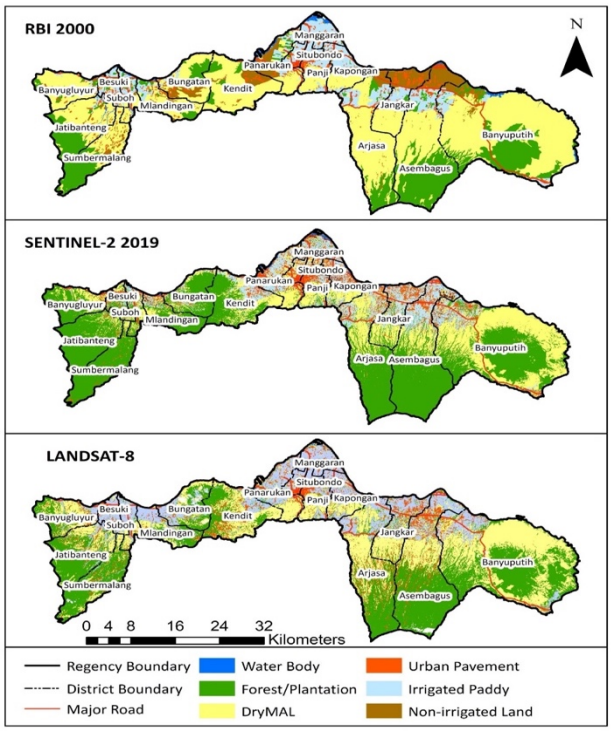

Fig. 5. Classified images from Sentinel-2A and Landsat 8 compared to the RBI map

government and stakeholders that have taken place between 2000 and 2019 has significantly changed LC and LU in this region. As a result, DryMAL resources have step-by-step been converted to more usable land occupation such as irrigated areas, forest/plantation and pavement areas. However, significant DryMAL areas (± 26.3% to ± 32.2% of the total area or ± 434.5 km^2 to ± 531.5 km^2) remain less usable during the prolonged dry seasons and efforts to increase the productivity of these DryMAL resources are urgently required.

Furthermore, pavement area has increased from 5.5% (in the RBI map) to 9.4% of the average total area (Table 5), meaning that during the last two decades (2000 to 2019) pavement area in the regency has almost doubled and is, therefore, occupying more land resources. This change has probably been caused by the rapid urbanisation and population growth of the city of Situbondo. The development of industrial and tourism sites along the coast has also increased pavement areas. The rapid conversion of agricultural land (both irrigated and non-irrigated) to urban or pavement areas has occurred in this regency, and this phenomenon has significantly appeared in the middle part of the map, around the city centre. Irrigated areas (appearing as blue areas in the RBI map) have also been converted to urban habitation or pavement areas. The result of this conversion appears in the Sentinel-2A and Landsat 8 maps as red (pavement), yellow (DryMAL) and blue (irrigated) areas. In this case, the statistical data, although obtained from the official bureau of statistics, is less valid for describing the development of urban pavement areas than the Landsat or Sentinel. The percentage (%) of urban pavement area obtained from the statistical data is ambiguous because it is less than the percentage in RBI The regional development initiated by the regency.

Table 5. Comparison of the areas from different sources

LCLU Class	RBI-map		BPS		Landsat 8		Sentinel-2A	
	km²	%	km²	%	km²	%	km²	%
Pavement area	90	5.5	89.8	5.4	154.1	9.3	157.0	9.5
DryMAL	859	52	347.0	21.0	531.5	32.2	434.5	26.3
Irrigated paddy	207	12.5	318.4	19.3	319.8	19.4	213.9	13.0
Non-irrigated land	109	6.6	114.3	6.9	0	0	17.5	1.1
Forest/plant-ation	363.3	22	763.7	46.3	638.3	38.7	818.0	49.5
Waterbody	23	1.4	18.1	1.1	7.6	0.5	10.3	0.6
Total	1651.3	100	1651.3	100	1651.3	100	1651.3	100

4.2 Evaluation of maps for specific districts

4.2.1 Arjasa

Arjasa is an example of a district in which DryMAL dominates. It is located in the eastern part of the regency and covers an area of 183.7 km^2. The change in DryMAL occupation is presented as in Table 6 and is visualised in **Fig. 6.**

Table 6. LCLU of Arjasa district

LCLU class	RBI-map		BPS		Landsat 8		Sentinel-2A	
	km²	%	km²	%	km²	%	km²	%
Pavement area	6.4	3.5	-	-	19.8	10.8	13.6	7.4
DryMAL	117.5	64.0	42.1	43.2	63.1	34.4	40.9	22.3
Irrigated paddy	22.4	12.2	29.5	30.3	27.7	15.1	22.0	12.0
Non-irrigated land	8.0	4.3	0.0	0.0	0.0	0.0	0.6	0.3
Forest-plantation	29	15.8	25.8	26.5	72.7	39.6	106.0	57.7
Waterbody	0.6	0.3	-	-	0.4	0.2	0.7	0.4
Total	183.7	100	97.5	100	183.7	100	183.7	100

In the RBI map presented in Fig. 6, DryMAL is shown in yellow and covers approximately 64% (117.5 km^2) of the total district area (Table 4) as at the year 2000. In the RBI map, landscape features are classified primarily by their utility (LU), while the Landsat 8 and Sentinel-2A distinguish features based on land cover (LC). The change in the land-resource occupation can be traced by focusing on two classes of land, i.e., DryMAL and forest-plantation. In the RBI map, these two classes occupied a land area of 117.5 km^2 + 29 km^2 respectively, totalling 146.5 km^2 or 79.8% of the total district area. This information is used to represent the original land resources in the region at the beginning of the 2000 period.

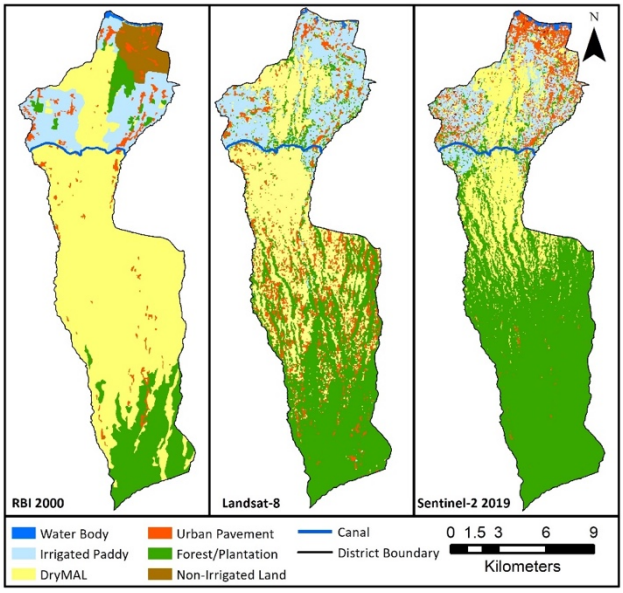

Fig. 6. Comparison of the classified maps of Arjasa district

Development between 2000 to 2019 has changed LCLU district, and both Landsat 8 and Sentinel-2A imagery can approximately capture these changes. The Landsat 8 map (Fig. 6 – middle image) measures the extent of DryMAL and forest-plantation as 63.1 km^2 + 72.7 km^2, respectively, totalling 135.8 km^2 or 74% of the district. The change is captured as an increase in the irrigated area identified below the canal, probably as a result of conversion from forest-plantation, non-irrigated land and pavement areas. In the Sentinel-2A map (final image in **Fig. 6**), the extent of DryMAL and forest-plantation is 40.9 km^2 + 106 km^2 respectively, totalling 146.9 km^2 or 80% of the area of the district (~ 79.8% in RBI map).

Both Landsat 8 and Sentinel-2A imageries captured pavement area of a relatively different extent (Table 3). Also, they describe the DryMAL, irrigated paddy and forest-plantation classes differently. The images captured at different points in the dry season. Sentinel-2A captured at the beginning of the season and Landsat 8 at the end. In consequence, Landsat 8 captured surface land cover that was drier overall than the Sentinel-2A images. The greenness of vegetation on the ground created by the recently ended wet-season captured in the Sentinel-2A images was therefore classified more frequently into the forest-plantation class. In contrast, the dry conditions at the end of the dry season were captured and classified more frequently by Landsat 8 as DryMAL, pavement or irrigated areas (Fig. 6).

The contour gradient in Arjasa follows a south-to-north direction, with altitude at the southern part of the district being higher than the northern part. The waterbody located at the northern edge is close to the coastline and is dominated by land resources used for the industrial culturing of shrimps and by traditional fishers.

The middle zone of the district, between the yellow and light-blue areas, is crossed by an irrigation canal constructed before the year 2000. The canal separates the irrigated area to the north and the DryMAL area to the south. The yellow zone below the canal line has a higher altitude than the canal itself, and therefore gravity irrigation cannot operate in this area. The canal can irrigate only about 12% to 13% of the district area. This division is mapped more precisely by Landsat 8 because it can separate more distinctly between annual vegetation (forest-plantation), waterbodies, pavement, irrigated areas and DryMAL. The non-irrigated area, in RBI-2000, appears as a brown area on the northern part is shown having been converted to the pavement and irrigated paddy.

DryMAL area decreased significantly between 2000 and 2019, showing that DryMAL had been converted to other types of useful occupation. In the lower-altitude zone (the northern area), DryMAL has been converted most frequently to built-up areas and irrigated and non-irrigated land. Meanwhile, in the higher-altitude zone (the southern area), DryMAL is occupied more for plantations (mango and coffee) and forested areas. During the last ten years, increasing numbers of mango trees have been planted to gain benefit from DryMAL areas. Both Landsat 8 and Sentinel-2A have difficulties in separating plantation and forested areas because the two features appear similarly as annual vegetation (permanent tree cover).

As the pixel size of Sentinel-2A is finer than Landsat 8, some features mapped are more fragmented, matching the reality that the landscape of the region is composed of a mixture of built-up areas, agricultural fields (both irrigated and non-irrigated) and annual vegetation cover. Therefore, the finer pixel resolution of Sentinel-2A can capture this fragmented landscape more precisely than Landsat 8.

4.2.2 Jatibanteng

The Jatibanteng district is located in the western part of the regency and covers an area of 104.8 km^2. LCLU change is observed as the increase in land resources used for plantation and forest. In contrast, DryMAL area has decreased significantly (Table 7).

Table 7. LCLU of Jatibanteng district

LCLU Class	RBI		BPS		Landsat 8		Sentinel-2A	
	km^2	%	km^2	%	km^2	%	km^2	%
Pavement area	3.8	3.7	No data		5.9	5.7	2.4	2.3
DryMAL	55.9	53.3	34.9	41.7	25.2	24.1	8.7	8.3
Irrigated paddy	3.3	3.1	6.3	7.5	7.9	7.5	0.9	0.9
Non-irrigated land	1.4	1.4	0.6	0.7	0.0	0.0	0.0	0.0
Forest - plantation	38.7	37.0	42.1	50.2	65.8	62.7	92.7	88.5
Waterbody	1.7	1.6	No data		0.0	0.0	0.0	0.0
Total	104.8	100			104.8	100	104.8	10

The RBI-2000 map classified LU into five primary classes: irrigated paddy, urban pavement, forest-plantation and waterbody. The irrigated areas are located in the northern part of the district. Then, DryMAL show in the middle zone and forest-plantation in the hilly zone. The waterbody area follows the river from the hilly to the flat area in the northern part (**Fig.7**).

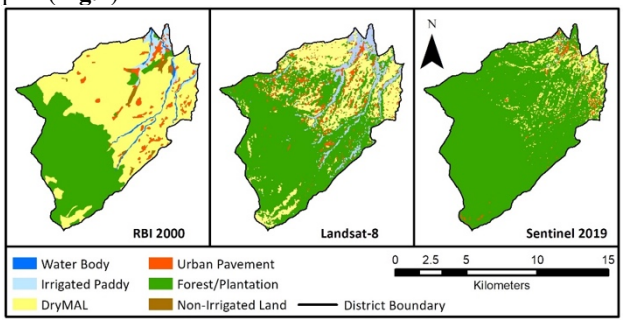

Fig. 7. Comparison of the classified maps of Jatibanteng district

In the Landsat 8, the homogenous zone of forest-plantation in the hilly area is accurately classified as a more homogenous zone. However, in the central area, the DryMAL shown in RBI-2000 is classified by Landsat 8 in a way that forms a more fragmented landscape composed of a mixture of DryMAL, irrigated, urban pavement and a few areas of annual vegetation. This is probably an accurate representation of nature but may also show an error generated by classification processes, with more DryMAL being classified as urban pavement and irrigated paddy. The Landsat 8 imagery tends to overestimate pavement and irrigated areas because its images were captured in September and October, at the end of the dry season, and ground surface condition in the dry season may create a similar spectral response to pavement areas.

In contrast, Sentinel-2A was captured at the end of the wet season (in June 2019) when the land cover was still dominated by vegetation. Sentinel-2A classified this land cover as being in the forest-plantation class. The western part of the regency in which Jatibanteng district is located is relatively wetter than the eastern part (Arjasa district). Sentinel-2A captured the end of the rainy season in which much vegetation had grown, and therefore more spectral response came from vegetation and was mapped accordingly. The statistical data obtained for this research was not satisfactory because it is difficult to obtain data about the extent of areas occupied by particular LCLU from such data.

This report shows that the use of satellite imagery provides up-to-date information on LCLU at the district level and that this free imagery can map changes in LCLU in simple, low-cost, up-to-date and accessible ways. The operator can handle the processing and production of mapping quickly and with basic knowledge of image-processing techniques.

5. Conclusions

This study demonstrates the use of Landsat 8 and Sentinel-2A imagery to map the spatial extent of DryMAL occupation for the year 2019. Supervised classification using a maximum likelihood algorithm can separate and distinguish primary land cover (i.e., DryMAL, pavement, irrigated-paddy, forest/plantation and waterbody). The results also show the change in LCLU from 2000 to 2019, observed as the increase in urban pavement and forest-plantation areas. This LCLU change has been compensated by the decrease in DryMAL, irrigated paddy areas, non-irrigated areas and water bodies. Positively, it can be seen that regional development has converted DryMAL resources to more beneficial uses. However, the remaining DryMAL is still unusable during the prolonged dry seasons. Both Landsat 8 and Sentinel-2A data can potentially apply for DryMAL and LCLU mapping of the region, and the maps produced from this research are also appropriate for updating incomplete statistical records.

References

1. K. S. Kuivanen, S. Alvarez, M. Michalscheck, S. Adjei-Nsiah, K. Descheemaeker, S. Mellon-Bedi, and J.C.J.Groota., "Characterising the diversity of smallholder farming systems and their constraints and opportunities for innovation: A case study from the Northern Region, Ghana," *NJAS - Wageningen J. Life Sci.*, vol. 78, pp. 153–166, Sept. 2016.
2. M. Von Cossel *et al.*, "Marginal agricultural land low-input systems for biomass production," *Energies*, vol. 12, no. 16. 2019.
3. W. Gerwin *et al.*, "Assessment and quantification of marginal lands for biomass production in Europe using soil-quality indicators," *SOIL*, vol. 4, no. 4, pp. 267–290, Dec. 2018.
4. D. Longato, M. Gaglio, M. Boschetti, and E. Gissi, "Accepted manuscript bioenergy and ecosystem services trade-offs and synergies in marginal agricultural lands: A remote-sensing-based assessment method," *J. Cleaner Production,* July 2019, https://doi.org/10.1016/j.jclepro.2019.117672.
5. A. Mulyani and M. Sarwani, "Karakteristik dan Potensi Lahan Sub Optimal Untuk Pengembangan Pertanian di Indonesia | Mulyani | Jurnal Sumberdaya Lahan," *J. Sumber d. Lahan*, vol. 7, no. 1, pp. 47–55, 2013.
6. P. P. dan P. T. dan Agroklimat, "Atlas Arahan Tata Ruang Pertanian Indonesia Skala 1:1.000.000.," Bogor, 2000.
7. A. Mulyani, A. Priyono, and F. Agus, "Semiarid soils of eastern Indonesia: Soil classification and land use," 2013, pp. 449–466, DOI: 10.1007/978-94-007-5332-7_24
8. EUROSTAT, "Manual of concepts on land cover and land use information systems," 2001.
9. T. E. Parece and J. B. Campbell, "Land use/land cover monitoring and geospatial technologies: An overview," pp. 1–32, 2015.
10. R. Eremiášová and H. Skokanová, "Land use changes (recorded in old maps) and delimitation of the most stable areas from the perspective of land use in the Kašperské Hory region," *J. Landsc. Ecol.*, vol. 2, no. 1, pp. 20–34, 2009.
11. M. Ptak and A. E. Ławniczak, "Changes in land use in the buffer zone of the lake of the Mała Wełna catchment," *Limnol. Rev.*, vol. 12, no. 1, pp. 35–44, 2012.
12. S. F. Fonji and G. N. Taff, "Using satellite data to monitor land-use land-cover change in north-eastern Latvia," *Springerplus*, vol. 3, no. 1, pp. 1–15, 2014.
13. R. A. Efroymson *et al.*, "A causal analysis framework for land-use change and the potential role of bioenergy policy," *Land Use Policy*, vol. 59, pp. 516–527, Dec. 2016.
14. X. Liu, W. Zhang, M. Wu, Y. Ye, K. Wang, and D. Li, "Changes in soil nitrogen stocks following vegetation restoration in a typical karst catchment," *L. Degrad. Dev.*, vol. 30, no. 1, pp. 60–72, Jan. 2019.
15. E. F. Moran, "Land cover classification in a complex urban-rural landscape with Quickbird imagery," *Photogramm. Eng. Remote Sensing*, vol. 76, no. 10, p. 1159, 2010.

16. P. Wężyk, P. Hawryło, M. Szostak, M. Pierzchalski, and R. De Kok, "Using Geobia and data fusion approach for land use and land cover mapping," *Quaest. Geogr.*, vol. 35, no. 1, pp. 93–104, 2016.
17. E. Bayramov, M. Buchroithner, and R. Bayramov, "Quantitative assessment of 2014–2015 land-cover changes in Azerbaijan using object-based classification of LANDSAT-8 time-series," *Model. Earth Syst. Environ.*, vol. 2, no. 1, Mar. 2016.
18. S. Mtibaa and M. Irie, "Land cover mapping in cropland dominated area using the information on vegetation phenology and multi-seasonal Landsat 8 images," *Euro-Mediterranean J. Environ. Integr.*, vol. 1, no. 1, Dec. 2016.
19. E. E. Hassen and M. Assen, "Land use/cover dynamics and its drivers in Gelda catchment, Lake Tana watershed, Ethiopia," *Environ. Syst. Res.*, vol. 6, no. 1, Jan. 2018.
20. Z. Bassa, U. Bob, Z. Szantoi, E. Commission, and R. Ismail, "Land cover and land use mapping of the iSimangaliso Wetland Park, South Africa: comparison of oblique and orthogonal random forest algorithms Zaakirah Bassa," vol. 10, Mar. 2016.
21. M.-R. Rujoiu-Mare, B. Olariu, B.-A. Mihai, C. Nistor, and I. Săvulescu, "Land cover classification in Romanian Carpathians and Subcarpathians using multi-date Sentinel-2 remote sensing imagery," *Eur. J. Remote Sens.*, vol. 50, no. 1, pp. 496–508, Jan. 2017.
22. G. Forkuor, K. Dimobe, I. Serme, and J. E. Tondoh, "Landsat-8 vs Sentinel-2: Examining the added value of Sentinel-2's red-edge bands to land-use and land-cover mapping in Burkina Faso," *GIScience Remote Sens.*, vol. 55, no. 3, pp. 331–354, May 2018.
23. A. M. Abdi, "Land cover and land use classification performance of machine learning algorithms in a boreal landscape using Sentinel-2 data," *GIScience Remote Sens.*, pp. 1–20, Aug. 2019.
24. T. Goga *et al.*, "A review of the application of remote sensing data for abandoned agricultural land identification with a focus on central and eastern Europe," *Remote Sensing*, vol. 11, no. 23, 2019.
25. R. H. Topaloğlu, E. Sertel, and N. Musaoğlu, "Assessment of classification accuracies of Sentinel-2 and Landsat-8 data for land cover/use mapping," in *International Archives of the Photogrammetry, Remote Sensing and Spatial Information Sciences - ISPRS Archives*, 2016, vol. 41, pp. 1055–1059.
26. P. K. Mishra, A. Rai, and S. C. Rai, "Land use and land cover change detection using geospatial techniques in the Sikkim Himalaya, India," *Egypt. J. Remote Sens. Sp. Sci.*, 2019.
27. D. K. Bolton, J. M. Gray, E. K. Melaas, M. Moon, L. Eklundh, and M. A. Friedl, "Continental-scale land surface phenology from harmonised Landsat 8 and Sentinel-2 imagery," *Remote Sens. Environ.*, vol. 240, Apr. 2020.
28. S. Khorram, S. A. C. Nelson, H. Cakir, and C. F. van der Wiele, "Digital image processing: Post-processing and data integration," in *Handbook of Satellite Applications*, vol. 2, New York: Springer, 2013, pp. 839–864.
29. S. Khorram, S. A. C. Nelson, H. Cakir, and C. F. van der Wiele, "Digital image acquisition: Preprocessing and data reduction BT" in *Handbook of Satellite Applications*," J. N. Pelton, S. Madry, and S. Camacho-Lara, Eds. New York, NY: Springer, 2013, pp. 809–837.
30. S. Khorram, S. A. C. Nelson, C. F. van der Wiele, and H. Cakir, "Fundamentals of Remote Sensing Imaging and Preliminary Analysis," in *Handbook of Satellite Applications*, New York, NY: Springer, 2016, pp. 1–36.
31. J. A. Richards, *Remote Sensing Digital Image Analysis: An Introduction*, vol. 9783642300622. Berlin Heidelberg: Springer Verlag, 2013.
32. G. M. Foody, "Thematic map comparison: Evaluating the statistical significance of differences in classification accuracy," *Photogramm. Eng. Rem. S.* vol. 70, no. 5. pp. 627–633, 2004.
33. G. M. Foody, "Status of land cover classification accuracy assessment," *Remote Sensing of Environment*, vol. 80, no. 1., pp. 185–201, 2002.
34. G. Foody, "Harshness in image classification accuracy assessment," *Int. J. Remote Sens.*, vol. 29, no. 11, pp. 3137–3158, Jun. 2008.
35. S. BPS, "Kabupaten Situbondo Dalam angka tahun 2019 (Regency Situbondo in number)," Situbondo, 2019.
36. U. S. G. USGS, "Landsat 8 (L8) Data Users Handbook Version 4.0," *Dep. Inter. U.S. Geol. Surv.*, vol. 4, p. 106, Apr. 2019.
37. BIG, "Indonesia Geospatial Portal," 2019. Online.. Available at: http://tanahair.indonesia.go.id/portal-web. Accessed: 15 Dec 2019..
38. D. Landgrebe and L. Biehl, "An Introduction & Reference For MultiSpec ©," 2011.
39. L. Biehl, "NEXUS Remote Sensing Workshop Intro to Remote Sensing using MultiSpec," 2018.
40. Q. D. Team, "QGIS Geographic Information System." Open Source Geospatial Foundation Project, 2019.
41. USGS, "EarthExplorer - Home," *U.S. Geological Survey*. 2019.
42. B. Johnson, R. Tateishi, and N. Hoan, "Satellite image pansharpening using a hybrid approach for object-based image analysis," *ISPRS Int. J. Geo-Information*, vol. 1, no. 3, pp. 228–241, Oct. 2012.
43. S. Khorram, S. A. C. Nelson, H. Cakir, and C. F. van der Wiele, "Digital image acquisition: Preprocessing and data reduction," in *Handbook of Satellite Applications*, vol. 2, New York: Springer, 2013, pp. 809–837.
44. D. Landgrebe, "MultiSpec Tutorial: Supervised Classification-Select Training Fields," 2015.